

Original Paper

Loss of heterozygosity at chromosome 9p21 is a frequent finding in enteropathy-type T-cell lymphoma

EC Obermann,¹ TC Diss,¹ RA Hamoudi,¹ P Munson,¹ BS Wilkins,² MLP Camozzi,³ PG Isaacson,¹ MQ Du¹ and A Dogan¹*

¹Department of Histopathology, University College London, UK

²Histopathology Department, Royal Victoria Infirmary, Newcastle upon Tyne, UK

³Instituto di Anatomica Patologica, Ospedale Niguarda Ca Granda, Milano, Italy

*Correspondence to:

A Dogan, MD, PhD, Department of Histopathology, University College London, Rockefeller Building, University Street, London WC1E 6JJ, UK.
E-mail: A.Dogan@ucl.ac.uk

Abstract

Enteropathy-type T-cell lymphoma (ETL) and ulcerative jejunitis (UJ) are rare disorders often occurring in patients with coeliac disease. The genetic events associated with the accumulation of intraepithelial lymphocytes in coeliac disease and tumour development are largely unknown. Deletions at chromosome 9p21, which harbours the tumour suppressor genes p14/ARF, p15/INK4b, and p16/INK4a, and 17p13, where p53 is located, are associated with the development and progression of lymphomas. To examine whether deletions at 9p21 and 17p13 play a role in ETL, 22 cases of ETL and seven cases of UJ were screened for loss of heterozygosity (LOH) by tissue microdissection and polymerase chain reaction (PCR) analysis for microsatellite markers. Furthermore, p53 and p16 protein expression was examined by immunohistochemistry. In addition, polymerase chain reaction–single strand conformational polymorphism (PCR–SSCP) analysis for detection of mutations in exons 5–8 of the p53 gene was performed in five cases of ETL and three cases of UJ. LOH was found in at least one microsatellite marker at the 9p21 locus in 8 of 22 (36%) ETLs, but not in UJ. Five of nine (56%) tumours composed of large cells showed LOH at 9p21, as opposed to two of eight (25%) tumours with small- or medium-sized cell morphology. The region spanning the p14/p15/p16 gene locus was most frequently affected (five cases); LOH at these markers coincided with loss of p16 protein expression in all of these cases. p53 overexpression was demonstrated in all ETLs examined and in four of seven cases of UJ. However, no alterations of the p53 gene were detected by LOH or PCR–SSCP analysis. The results of this study show that LOH at chromosome 9p21 is frequent in ETL, especially in tumours with large cell morphology; this finding suggests that gene loss at this locus may play a role in the development of ETL. Copyright © 2004 John Wiley & Sons, Ltd.

Keywords: enteropathy-type T-cell lymphoma; ulcerative jejunitis; loss of heterozygosity; chromosome 9; chromosome 17; p15/INK4b; p16/INK4a; p14/ARF; p53

Received: 8 April 2003
Revised: 4 July 2003
Accepted: 27 October 2003

Introduction

Enteropathy-type T-cell lymphoma (ETL) is an extra-nodal non-Hodgkin's lymphoma, which was first described by Isaacson and Wright as a single entity [1] and later shown to be of T-cell lineage [2]. ETL may occur in patients with a history of coeliac disease that does not respond to gluten withdrawal, a condition known as refractory sprue. Refractory sprue does not always lead to the development of ETL with an overt tumour and is sometimes complicated by intestinal ulceration [ulcerative jejunitis (UJ)], similar to that seen in the non-lymphomatous mucosa in ETL. Molecular investigations show that refractory sprue and UJ are characterized by a monoclonal T-cell population that is linked to the subsequent tumour [3,4]. It has been suggested that refractory sprue and UJ are cryptic T-cell lymphomas [5].

A broad spectrum of histopathological appearances of the tumours in ETL has been described. It has

been suggested that ETLs should be divided into two categories based on their morphology. One category consists of tumours with pleomorphic small or monomorphic medium-sized cells. The tumours composed of pleomorphic small cells consist of cells with irregular nuclei and clear cytoplasm. For tumours with monomorphic medium-sized cells, a monotonous appearance at both low- and high-power magnification is typical. Another category encompasses tumours composed of pleomorphic medium- to large-sized cells and tumours composed of large cells which show either immunoblastic or anaplastic features [6]. In addition, a purely intraepithelial form of ETL with a 'low-grade' intraepithelial tumour population displaying an abnormal immunohistochemical phenotype and a clonal T-cell receptor rearrangement has been identified and termed epitheliotropic lymphoma [7], cryptic ETL [8,9] or IEL lymphoma [10]. Neoplastic cells are mostly CD3+, CD4-, CD8- and contain cytotoxic granules [11].

Although progress has been made in clarifying the clinicopathological features of ETL and UJ, little is known about the underlying genetic alterations. Epstein–Barr virus has been found in some cases of ETL, but its aetiological relevance is questionable [12,13]. By immunohistochemistry, p53 protein overexpression has been observed in one study of ETL, but whether this is the result of somatic mutations of the p53 gene remains unclear [14]. Recently, the first comprehensive survey of genetic alterations in ETL using comparative genomic hybridization (CGH) and fluorescence *in situ* hybridization (FISH) showed recurrent chromosomal gains and losses. Gains of chromosome 9q34 were most frequently encountered, while losses were found at 13q, 8p, and 9p, the latter with a minimal overlapping region at 9p21 [15]. Interestingly, deletions of chromosome 9 demonstrated by karyotypic analysis in ETL were reported as early as 1991 [7].

The most commonly altered tumour suppressor genes in human cancer are p15/p16, located on 9p21, and p53, located on 17p13. p15 and p16 are inhibitors of cyclin-dependent kinases 4 and 6, contributing to G1 arrest by blocking retinoblastoma protein (RBP) phosphorylation [16]. There is evidence that p16 is targeted in most tumours with deletions at 9p21 [17]. Another tumour suppressor gene, p14/ARF — also located on chromosome 9p21 — is closely linked to p16/INK4a. p14 has a different first exon from p16, designated exon 1 β , which splices into exon 2 of the p16 gene in an alternative reading frame, resulting in a distinct transcript. The expression of p14 and p16 is controlled by independent promoters [18]. p14 binds specifically to MDM2, resulting in the stabilization of p53 [19,20]. The fact that the p15/p16–CDK4/6–RBP and the p14–MDM2–p53 pathways are intimately linked on chromosome 9p21 makes this locus especially interesting. Alterations at 9p21 are associated with the development and progression of T- and B-cell lymphomas, such as mycosis fungoides [21] and follicular lymphoma [22].

To examine whether deletions at 9p21 and 17p13 play a role in the development of ETL, we screened these loci for LOH in 22 cases of ETL and seven cases of UJ by microdissection and PCR analysis of microsatellite markers. To assess the functional significance of genetic changes at the locus 9p21, p16 protein expression was studied using immunohistochemistry. We also investigated p53 gene mutation and protein overexpression by polymerase chain reaction–single strand conformation polymorphism (PCR–SSCP) and immunohistochemistry, respectively.

Materials and methods

Patient and specimen selection

Local ethical guidelines were followed for this study. Forty-five cases of ETL and UJ were retrieved from

the files of the Department of Histopathology, University College London. Twenty-two cases were selected for this study. The remaining cases did not meet the criteria selected (histopathological review by at least two histopathologists, monoclonal T-cell receptor gene rearrangement) or the material was insufficient for further analysis. The ETL patients fell into two categories. One category (T-ETL) consisted of 17 patients with a mass lesion of the small intestine (nine males, average age 62 years, range 32–82 years; eight females, average age 65 years, range 42–88 years). The other category contained five patients (two male, average age 47 years; three females, average age 58 years); here, ETL consisted entirely of an intra-epithelial component without an overt tumour (IEL-ETL). Of the patients with UJ, three were male (average age 76 years) and four were female (average age 62 years).

In 16 cases of T-ETL, one case of IEL-ETL, and six cases of UJ investigated by LOH, the tissue came from surgical resection specimens. In one case, tissue was obtained during autopsy. In the remaining cases, tissue samples were biopsies. In addition, paraffin wax-embedded material from 16 lymphomas (peripheral T-cell lymphoma/not otherwise specified: eight cases; angioimmunoblastic T-cell lymphoma: four cases; peripheral T-cell lymphoma/lymphoepithelioid variant (Lennert lymphoma): one case; precursor T-lymphoblastic lymphoma: one case; anaplastic large cell lymphoma: two cases) and five tissue samples containing non-neoplastic lymphatic cells (one lymph node; two cases with lymphoid hyperplasia of the intestine) were included in the study. The histological features of all cases were reviewed by at least two pathologists (EO, AD, MC, BW, PI); all cases were classified according to the current World Health Organization classification of tumours of haematopoietic and lymphoid tissue [23].

Immunohistochemistry

Immunohistochemical analysis was performed on formalin-fixed, paraffin wax-embedded sections for the following markers: CD3 (dilution 1:400, DAKO), CD4 (1:800, Novocastra), CD5 (1:100, Novocastra), CD8 (1:50, DAKO), CD20 (1:400, DAKO), CD56 (1:30, Monozym), CD30 (1:40, DAKO), TIA-1 (1:500, Coulter), p53 (1:100, DAKO), and p16 (1:250, Novocastra) according to standard protocols. Appropriate controls were used for all markers.

The degree of immunopositivity for p53 was evaluated using a scoring system for both the extent and the intensity of p53 staining. The extent of staining was classified into five categories according to the number of stained cells in relation to all neoplastic cells (<5%, 5–25%, 26–50%, 51–75%, >75%). The intensity of p53 staining was graded as 0, +1, +2 or +3. Overexpression of p53 was assumed when the number of tumour cells expressing p53 exceeded 4% of all tumour cells, independently of staining intensity. In

UJ, where the ulcers do not show any obvious tumour cells, the intraepithelial lymphocytes in the adjacent epithelium were evaluated.

p16 protein expression was assessed by evaluating p16 staining in the nuclei of neoplastic cells. Only predominantly nuclear activity was considered as a positive signal. Samples were scored 'negative' and functionally significant loss of p16 protein was assumed if less than 10% of neoplastic cells had retained p16 expression. This cut-off value has been described previously [22].

Microdissection and DNA extraction

For microdissection, 10 µm sections on glass slides were dewaxed with xylene, rinsed in ethanol from 100% to 70%, and stained with haematoxylin. Microdissection was performed by hand under direct light microscopic visualization (×40 magnification) using a 22-gauge needle. Consecutive sections were stained with haematoxylin and eosin (H&E) and antibodies against CD3 to identify the relevant lesions.

In IEL-ETL, epithelium densely infiltrated by neoplastic cells was microdissected. In UJ, either the intraepithelial component or/and the base of the ulcers was microdissected, depending on the presence of CD3+ cells. In 11 T-ETLs, it was possible to microdissect both the tumour lesion and the neoplastic intraepithelial component. In one case (case 14), intraepithelial cells from both the immediate proximity of the tumour and the resection margin were taken. In another case (case 21), tumour cells disseminated to a regional lymph node were also microdissected (Table 1). To ensure a sufficiently high content of neoplastic cells for LOH analysis, only areas with more than 80% tumour cells were microdissected. These cells were digested with 200 µg/ml proteinase K in a 40–200 µl PCR buffer solution at room temperature for 12–18 h. Proteinase K was inactivated at 95 °C for 15 min. Cell debris was pelleted by centrifugation and the supernatant was used for PCR. Normal DNA as a reference for LOH analysis was isolated from microdissected non-neoplastic tissue such as lamina muscularis propria in intestinal resection specimens, submucosa in biopsies, or perinodal fat and connective tissue in lymph node specimens.

Single-strand conformation polymorphism (SSCP) analysis

Five cases of T-ETL (cases 16, 18, 23, 26, and 27) and three cases of UJ (cases 1, 3, and 6) were analysed for mutations of the p53 gene. Because the majority of mutations of p53 occur in exons 5, 6, 7, and 8, these exons were investigated by PCR–SSCP as described previously [24]. Briefly, PCR was performed using a hot-start protocol with an initial denaturation step at 94 °C for 5 min, 40 cycles consisting of a denaturation step at 94 °C for 30 s, an annealing step at 58 °C for 30 s, and an extension step at 72 °C for 60 s, followed

by a final extension at 72 °C for 5 min. For SSCP, 2 µl of PCR product was mixed with 4 µl of loading buffer, denatured, separated on a Genephor electrophoresis system (Pharmacia-Amersham) under 15 W constant power for 2–3 h at 5 °C, and then visualized by silver staining. Primer sequences and the lengths of their respective products are listed in Table 2.

Clonality analysis

Clonality analysis of the T-cell receptor γ chain (TCR- γ) gene was carried out in all malignant cases to ensure that the microdissected tumour samples contained neoplastic cells and were therefore representative for genetic analysis. PCR amplification of TCR- γ was carried out using an adapted protocol with five different primers in two reactions as described previously [25]. The primer sets were altered by the addition of a V γ II primer (5' to 3' sequence: GAGAAACAGGACATAGCTAC) to each reaction [26]. PCR products were run on a 10% polyacrylamide gel, stained with ethidium bromide, and visualized under ultraviolet light. In each experiment, a positive control T-cell lymphoma and a negative control without DNA were run in parallel.

LOH analysis

Twelve microsatellites with a dinucleotide repeat were used to examine the 9p21 locus. The markers targeted were IFNa, D9S1751, D9S1749, D9S1747, p15/p16 marker, D9S1748, D9S1604, D9S1752, D9S958, D9S171, D9S169, and D9S161 in an order from telomere to centromere. For the evaluation of p53, one marker located on chromosome 17p13 was used. All markers apart from the p53 marker [27], IFNa, p15/p16 marker, and D9S171 [28] were identified from the second-generation linkage map constructed by the Genethon group [29]. The p15/p16 marker, which is located between the p15 and the p16 gene, was redesigned to shorten the length of the resulting PCR product. For primer design, 'primer 3' software from the Whitehead Institute/Center for Genome Research, Cambridge, MA, USA and 'oligos' software from the Biocentre of the University of Helsinki, Finland were used. One primer from each pair was fluorescently labelled using either FAM dye, HEX dye, or NED dye (Applied Biosystems).

DNA was amplified by PCR with conditions optimized for each primer pair. The different reaction mixes consisted of 200 µM each dNTP, 1× PCR buffer (Invitrogen), 0.375 unit of Taq polymerase (Platinum Taq DNA Polymerase, Invitrogen), 5 mM MgCl₂, 10 µg of each primer, and 0.5 µl (reaction mix 1) or 1.0 µl (reaction mix 2) of extracted DNA template in a total volume of 25 µl.

DNA was amplified by one of the three touch-down PCR programs in a thermal cycler (Hybaid, Omnigene). A typical cycle consisted of a denaturation step of 93 °C for 30 s, an annealing step at 60 °C for

Table 1. LOH at chromosome 9p21, p53 analysis, and p16 protein expression

No	Diagnosis	L	IFNa	LOH analysis at chromosome 9p21										p53 analysis			p16 IHC		
				D9S1751	D9S1749	D9S1747	p15/p16	D9S1748	D9S1604	D9S1752	D9S958	D9S171	D9S169	D9S161	LOH p53	% Intensity			
1	Uj	IEL	—	—	—	—	—	—	—	—	—	—	—	—	—	—	< 5	0	P
2	Uj	IEL	—	—	—	—	—	—	—	—	—	—	—	—	—	—	< 5	0	P
3	Uj	U	—	—	—	—	—	—	—	—	ni	—	—	—	—	—	5–25	1	na
4	Uj	IEL	—	—	ni	—	—	—	—	—	ni	—	—	—	—	—	5–25	2	na
5	Uj	U/IEL	—	—	—	—	—	—	—	—	f(t)	—	—	—	—	—	26–50	1	n
6	Uj	IEL	—	f(t)	—	—	—	—	—	—	—	—	—	—	—	—	< 5	0	P
7	Uj	IEL	—	f	—	—	—	—	—	—	f(t)	—	—	—	—	—	< 5	0	P
8	IEL-ETL*	U	—	—	—	—	—	—	—	—	—	—	—	—	—	—	26–50	1	n
9	IEL-ETL*	IEL	—	—	—	—	—	—	—	—	—	—	—	—	—	—	26–50	1	n
10	IEL-ETL	IEL	—	—	—	—	—	—	—	—	—	—	—	—	—	—	26–50	1	n
11	IEL-ETL	IEL	—	—	—	—	—	—	—	—	—	—	—	—	—	—	50–75	2	P
12	IEL-ETL	IEL	—	—	—	—	—	—	—	—	—	—	—	—	—	—	50–75	2	P
13	T-ETL (s)*	T	—	—	—	—	—	—	—	—	—	—	—	—	—	—	50–75	2	P
14	T-ETL (s)*	IEL	—	—	—	—	—	—	—	—	—	—	—	—	—	—	50–75	2	n
15	T-ETL (s)*	IEL	—	—	—	—	—	—	—	—	—	—	—	—	—	—	26–50	1	na
16	T-ETL (s)*	IEL	—	—	—	—	—	—	—	—	—	—	—	—	—	—	> 75	2	na
17	T-ETL (s)	T	—	—	—	—	—	—	—	—	—	—	—	—	—	—	< 5	0	na
18	T-ETL (s)	IEL	—	—	—	—	—	—	—	—	—	—	—	—	—	—	26–50	2	P
19	T-ETL (m)	IEL	—	f	—	—	—	—	—	—	—	—	—	—	—	—	5–25	1	P
20	T-ETL (m)	T	—	—	—	—	—	—	—	—	—	—	—	—	—	—	26–50	1	P
21	T-ETL (m/l)	IEL	—	—	—	—	—	—	—	—	—	—	—	—	—	f	na	na	na
22	T-ETL (m/l)	T	—	—	—	—	—	—	—	—	—	—	—	—	—	—	50–75	2	P
23	T-ETL (l)	IEL	—	—	—	—	—	—	—	—	—	—	—	—	—	—	26–50	1	P
24	T-ETL (l)	T	—	—	—	—	—	—	—	—	—	—	—	—	—	—	5–25	1	n
		IEL	—	—	—	—	—	—	—	—	—	—	—	—	—	—	< 5	0	P
		IEL	—	—	—	—	—	—	—	—	—	—	—	—	—	—	50–75	2	P
		IEL	—	—	—	—	—	—	—	—	—	—	—	—	—	—	50–75	2	P
		D	—	—	—	—	—	—	—	—	—	—	—	—	—	—	50–75	2	na
		T	—	—	—	—	—	—	—	—	—	—	—	—	—	—	5–25	2	P
		IEL	—	—	—	—	—	—	—	—	—	—	—	—	—	—	5–25	1	P
		T	—	—	—	—	—	—	—	—	—	—	—	—	—	—	50–75	2	P
		IEL	—	—	—	—	—	—	—	—	—	—	—	—	—	—	50–75	1	P
		IEL	—	—	—	—	—	—	—	—	—	—	—	—	—	—	50–75	1	P

Table 1. Continued

Case details		LOH analysis at chromosome 9p21											p53 analysis					
		LOH	D9S161	D9S169	D9S171	D9S172	D9S1752	D9S1748	D9S1748	D9S1748	D9S1747	p15/p16	IHC	IHC	p16			
No	Diagnosis	L	IFNa	D9S1751	D9S1749	D9S1747	p15/p16	D9S1748	D9S1604	D9S1752	D9S958	D9S171	D9S169	D9S161	LOH	%	Intensity	IHC
25	T-ETL(i)	T	—	—	—	—	—	—	—	—	—	—	—	—	—	26–50	1	p
26	T-ETL(a)	IEL	—	—	ni	—	—	—	—	—	—	—	—	—	—	26–50	1	p
27	T-ETL(a)	IEL/U	—	—	—	—	—	—	—	—	LOH	—	—	—	—	5–25	1	p
28	T-ETL(a)	T	—	—	—	—	ni	—	—	—	—	—	LOH	—	—	> 75	2	p
29	T-ETL(a)	IEL	—	—	—	—	—	—	—	—	—	—	—	—	—	50–75	2	p
30	PTL	T	—	—	—	—	—	LOH	—	—	—	—	—	—	—	5–25	1	p
31	PTL	T	—	—	—	—	—	LOH	—	—	—	—	—	—	—	5–25	1	p
32	PTL	T	—	—	—	—	—	LOH	—	—	—	—	—	—	—	50–75	2	p
33	PTL	T	—	—	—	—	—	LOH	—	—	—	—	—	—	—	50–75	2	p
34	PTL	T	—	—	—	—	—	LOH	—	—	—	—	—	—	—	50–75	2	p
35	PTL	T	—	—	—	—	—	LOH	—	—	—	—	—	—	—	50–75	2	p
36	PTL	T	—	—	—	—	—	LOH	—	—	—	—	—	—	—	50–75	2	p
37	PTL	T	—	—	—	—	—	LOH	—	—	—	—	—	—	—	50–75	2	p
38	AITL	T	—	—	—	—	—	LOH	—	—	—	—	—	—	—	50–75	2	n
39	AITL	T	—	—	—	—	—	LOH	—	—	—	—	—	—	—	50–75	2	n
40	AITL	T	—	—	—	—	—	LOH	—	—	—	—	—	—	—	50–75	2	n
41	AITL	T	—	—	—	—	—	LOH	—	—	—	—	—	—	—	50–75	2	n
42	PTL/LL	T	—	—	—	—	—	LOH	—	—	—	—	—	—	—	50–75	2	n
43	PTL/LL	T	—	—	—	—	—	LOH	—	—	—	—	—	—	—	50–75	2	n
44	ALCL	T	—	—	—	—	—	LOH	—	—	—	—	—	—	—	50–75	2	n
45	ALCL	T	—	—	—	—	—	LOH	—	—	—	—	—	—	—	50–75	2	n
46	LN	LT	—	—	—	—	—	LOH	—	—	—	—	—	—	—	50–75	2	n
47	LH	LT	—	—	—	—	—	LOH	—	—	—	—	—	—	—	50–75	2	n
48	LH	LT	—	—	—	—	—	LOH	—	—	—	—	—	—	—	50–75	2	n

* CD56-positive. UJ = ulcerative jejunitis; IEL-ETL = intraepithelial ETL; T-ETL = ETL with overt tumour; L = lesion used for evaluation/microdissection; IHC = immunohistochemistry; T = tumour; U = ulcer; IEL = intraepithelial lymphocytes; (c) = IEL close to tumour; (d) = IEL distant from tumour; D = dissemination; LT = non-neoplastic lymphatic tissue; PTL = peripheral T-cell lymphoma/unspecified; AITL = angioimmunoblastic T-cell lymphoma; PTL/LL = peripheral T-cell lymphoma/lymphoepithelioid variant (Lennert lymphoma); PTLBL = precursor T-lymphoblastic lymphoma; ALCL = anaplastic large cell lymphoma; LN = lymph node; LH = lymphatic hyperplasia; (s) = small-sized cell type; (m) = monomorphic medium-sized cell type; (m/l) = medium to large-sized cell type; (i) = immunoblastic cell type; (a) = anaplastic cell type; LOH = loss of heterozygosity; f = failed DNA-amplification; f(t) = failed amplification in tumour sample; ni = non informative; — = informative, but no LOH; na = not available; p = positive, ie p16 expression in more than 10% of neoplastic cells; n = negative, ie p16 expression in less than 10% of neoplastic cells.

Table 2. LOH and PCR–SSCP analyses

Microsatellite markers used for LOH analysis			Estimated size (bp)	Dye	Reaction mix	PCR program
Marker	Forward primer (5' to 3')	Reverse primer (5' to 3')				
IFN- α	TGCGCGTTAAGTTAATTGGTT	GTAAGGTGGAACCCCTACT	146	HEX	1	3
D9S1751	TTGTTGATTCTGCCTTCAAAGTCTTTTAAAC	CGTTAAGTCCTCTATTACACAGA	170	FAM	2	2
D9S1749	AGGAGAGGGTACGCTTGCA	TACAGGGTGCGGGTGCAGATAA	160	HEX	2	2
D9S1747	ATTCAACGAGTGGGATGAAG	TCCAGTTGCTGCAAAATGCC	150	FAM	1	3
p15/p16	CCGCAGGCAGACTACACAG	CATAAGGGGATTTCCGCATC	142	FAM	1	3
D9S1748	CACCTCAGAAATCAGTGAGT	GTGCTTGAAATACACCTTTCC	150	NED	1	1
D9S1604	CCTGGGTCTCCAATTTGTCA	AGCACATGACACTGTGTGTG	175	NED	1	1
D9S1752	AGACTACACAGGATGAGGTG	GCAAGTCATAAGGGGATTTTC	160	NED	1	3
D9S958	GTTCCGCAGGCAGACTACAC	CATAAGGGGATTTCCGCATC	182	FAM	1	1
D9S171	AGCTAAGTGAACCTCATCTGTCT	ACCCTAGCACTGATGGTATAGTCT	177	HEX	2	2
D9S169	AGACAGATCCAGATCCCCTG	GGGGGTTAGTTCTTTCTGAT	186	FAM	1	1
D9S161	TGCTGCATAACAAATTACCAC	CATGCCTAGACTCCTGATCC	135	FAM	1	1
p53-marker	AGGGATACTATTAGCCCGAGGTG	ACTGCCACTCCTTGCCCCATTTC	135	FAM	1	1

Primers used for PCR–SSCP			Estimated size (bp)
p53 gene	Forward primer (5' to 3')	Reverse primer (5' to 3')	
Exon 5	TTCTCTTCTGCAGTACTC	ACCCTGGGCAACCAGCCCTGT	245
Exon 6	AGTTGCAAACCAGACCTCAG	ACAGGGCTGGTTGCCAGGGT	163
Exon 7	GTGTTGCCTCCTAGGTTGGC	CAAGTGGCTCCTGACCTGGA	138
Exon 8	CCTATCCTGAGTAGTGATAA	GTCCTGCTTGCTTACCTCGC	166

45 s, and an elongation step at 72 °C for 1.5 min. The initial denaturation was either 95 °C for 2 min (programs 1 and 2) or 5 min (program 3); the final extension was at 72 °C for 5 min for all programs. The annealing temperature of 60 °C was stepwise reduced by 1 °C to 50 °C (programs 2 and 3) or to 55 °C (program 1), followed by 40 cycles with an annealing temperature of 50 °C (programs 2 and 3) or 55 °C (program 1). The primer sequences, estimated lengths of the PCR products, dyes, the relevant reaction mixes, and PCR programs for each primer pair are listed in Table 2.

For LOH detection, PCR products with different fluorescent dyes were mixed and analysed on an ABI 377 automated DNA sequencer using the GeneScan mode (Applied Biosystems, CA, USA). The data collected were automatically analysed with the GeneScan Analysis Software (version 3.1) (Applied Biosystems, CA, USA). Each fluorescent peak was calculated in terms of peak height and peak area. To determine whether LOH was present in a case, comparison of the ratios between neoplastic and normal samples was carried out. The formula employed for the calculation was $T1 : T2/N1 : N2$, where T1 and N1 are the peak heights of one of the alleles and T2 and N2 are the peak heights of the others. For ratios greater than 1, the reciprocal of the ratio was calculated to give a figure between 0.0 and 1.0. LOH was only recorded if the ratio of 'neoplastic' to 'normal' alleles was less than 0.25. This strict approach has been described previously [30].

Results

Histopathology, immunophenotyping, and TCR- γ analysis

Among the 17 ETLs with an overt tumour, eight cases (47%) showed pleomorphic small-sized (cases

13–17) or monomorphic medium-sized (cases 18–20) tumour cells; the remaining nine cases displayed a large cell morphology (cases 21 and 22 with pleomorphic medium-sized to large tumour cells; cases 23–25 with immunoblastic cells; and cases 26–29 with anaplastic features). Five ETLs (cases 8–12) consisted purely of intraepithelial neoplastic cells without clinical or histopathological evidence of a tumour mass, but a marked increase of intraepithelial lymphocytes with an abnormal immunophenotype (CD3+, CD4–, CD5–). In two of these cases (cases 8 and 9), the neoplastic cells expressed CD56.

In UJ, an increase of intraepithelial lymphocytes was found in the epithelium adjacent to the areas of mucosal ulceration and no overt tumour mass was present. For assessment of the immunophenotype, the intraepithelial cells were evaluated. None of the cases of UJ showed neoplastic cells positive for CD56 in either the intraepithelial compartment or the ulcerated areas (Table 1).

All cases of ETL and UJ examined were negative for CD4, CD5, and CD20. In one case (case 20), CD3 was negative in the main tumour, but positive in the accompanying intraepithelial cells and partly positive in two other cases (cases 18 and 24). All the other cases expressed CD3 uniformly. CD30 was positive in two tumours (cases 24 and 29). The cytotoxic marker TIA-1 was expressed in 11 of 15 evaluated T-ETLs (73%) (cases 13, 14, 16, 17, 19–21, 24–26, and 29), three of five IEL-ETLs (60%) (cases 8, 10, and 12), and four of five UJ (80%) (cases 3–6).

Loss of p16 expression (ie <10% of neoplastic cells showed nuclear positivity for p16) was found in two of five cases of UJ, one of four cases of IEL-ETL, and four of 16 evaluated T-ETLs. In two of the latter cases, loss of p16 protein expression was found in

both the tumour and the intraepithelial component; in the other two cases, lack of p16 protein was only noted in the overt tumour. All five cases of ETL with LOH in the region covered by the microsatellite markers D9S1747, p15/p16, D9S1748, and D9S1604 showed lack of p16 expression (Figure 1). On the other hand, none of the overt tumours with LOH at different microsatellite markers showed lack of p16 protein expression.

T-cell clonality was investigated by PCR analysis of the rearranged TCR- γ gene. Monoclonality was demonstrated in the microdissected tumour samples of all cases of ETL and UJ and in nine other lymphomas (cases 30–34 and 38–41). In seven cases of non-ETL lymphomas (cases 35–37 and 42–45), neither the microdissected tumour samples nor a whole tissue section showed monoclonality; these cases were included in this study based on strict histopathological criteria.

p53 analysis

Immunohistochemistry for p53 protein was performed in seven cases of UJ and 21 ETLs. Overexpression was found in 16 T-ETLs. The percentage of positive neoplastic cells in T-ETL was 5–25% in 5 of 16 cases (31%), 26–50% in four cases (25%), 51–75% in

five cases (31%), and greater than 75% in two cases (13%). The intensity of the staining ranged between +1 (eight cases, 50%) and +2 (eight cases, 50%). The corresponding intraepithelial component showed the same extent and intensity of staining except in five cases, in which both the extent and the intensity were lower than in the tumour. No clear correlation was found between tumour morphology and extent or intensity of p53 protein expression.

In IEL-ETL, two of five cases expressed p53 protein in 26–50% of all tumour cells with an intensity of +1, while the three remaining cases showed expression in 51–75% of cells with an intensity of +2. In UJ, p53 accumulation was found in four of seven cases examined, with 5–25% of neoplastic intraepithelial cells positive in two cases and 26–50% of neoplastic cells positive in the remaining two cases (Table 1 and Figure 1).

PCR–SSCP for exons 5, 6, 7, and 8 of the p53 gene was performed in eight cases. DNA could not be amplified for exon 8 in one case (case 23). PCR–SSCP showed no altered electrophoretic mobility, despite the fact that the detection system has been shown to be highly sensitive in screening for gene mutations previously [24].

LOH analysis of the p53 gene was carried out in 45 neoplastic cases and three non-neoplastic control

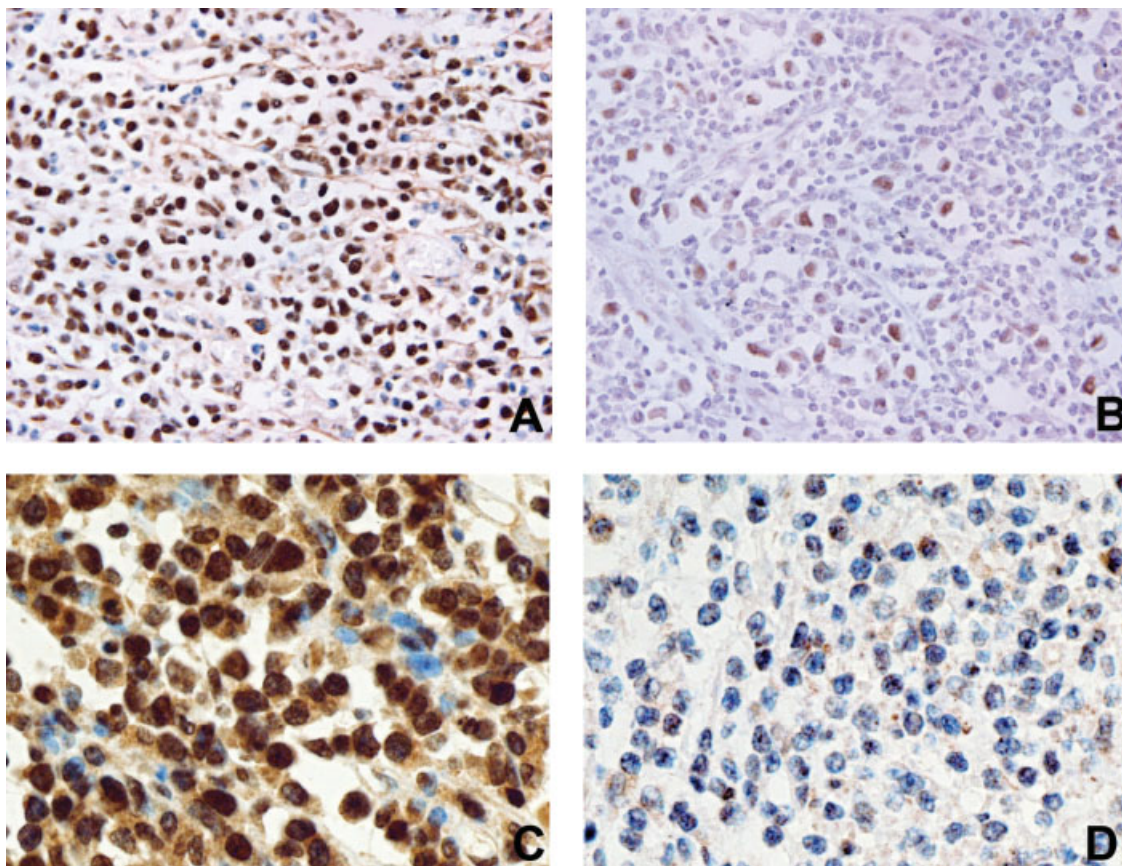


Figure 1. p53 protein staining. (A) Enteropathy-type T-cell lymphoma with expression of p53 protein in 50–75% of tumour cells, intensity +2 (case 21). (B) Enteropathy-type T-cell lymphoma with expression of p53 protein in 5–25% of tumour cells, intensity +1/+2 (case 22). (C) Enteropathy-type T-cell lymphoma with expression of p16 protein in most tumour cells; note the occasional negative stromal cell (case 21). (D) Enteropathy-type T-cell lymphoma lacking p16 protein expression (case 13)

cases. All cases in which DNA could be amplified were heterozygous for the p53 CA repeat and thus informative. However, LOH was not encountered in any of these cases (Table 1).

LOH on chromosome 9p21

LOH analysis at the 9p21 locus was performed in 45 neoplastic and three non-neoplastic cases. Eight of 22 (36%) ETLs demonstrated LOH for at least one microsatellite marker at 9p21. This included 7 of 17 T-ETLs (41%) and one of five (20%) IEL-ETLs. In one T-ETL (case 29), LOH at D9S1748 was encountered in both the tumour sample and the ulcerated component; in the remaining cases, LOH could only be demonstrated in the tumour samples, but not in the intraepithelial components. Of the four patients with a CD56+ tumour, one (25%) had LOH at 9p21 (case 10); the two patients with a CD56+ IEL-ETL displayed no LOH. Of the eight cases of T-ETL with small- or medium-sized cell morphology, two (25%) showed LOH at 9p21 (cases 13 and 20). Within the category of tumours with large cell morphology, LOH was encountered in five of nine (56%) cases. In tumours consisting of anaplastic cells, LOH was found in three of four cases (cases 27–29). In the fourth case with an anaplastic tumour (case 26), no material from the tumour itself was available for LOH analysis; therefore the intraepithelial component/base of ulceration was evaluated. In five patients, LOH was encountered in the region covered by the markers D9S1604, D9S1748, p15/p16 marker, and D9S1747.

LOH at D9S161 and D9S169 was found in two patients each. LOH was not found in any case of UJ. Furthermore, three cases of other lymphoma entities showed LOH at one microsatellite marker each. Two of these were angioimmunoblastic T-cell lymphomas (cases 38 and 39) and one was a peripheral T-cell lymphoma/lymphoepithelioid cell variant (Lennert lymphoma) (case 42). Eight neoplastic cases showed failure of PCR from tumour cells, but not from non-neoplastic tissue. For validation of the methodology, five tissue samples without malignant alterations were examined. None of these samples showed LOH at any marker (Table 1 and Figure 2).

Discussion

Investigations into the immunophenotype and T-cell clonality analyses of ETL, UJ, refractory sprue, and coeliac disease have shown that the accumulation of immunophenotypically aberrant, monoclonal intraepithelial lymphocytes is an early step in the development of ETL. However, few data are available on genetic changes in UJ and ETL. Recently, CGH revealed genetic imbalances in 87% of ETLs analysed, the most striking finding being recurrent gains at chromosome 9q. In addition, an interesting observation was a recurrent loss of genetic material in 18% of cases at chromosome 9p with the minimal overlapping region at 9p21, where the tumour suppressor genes p14, p15, and p16 are located.

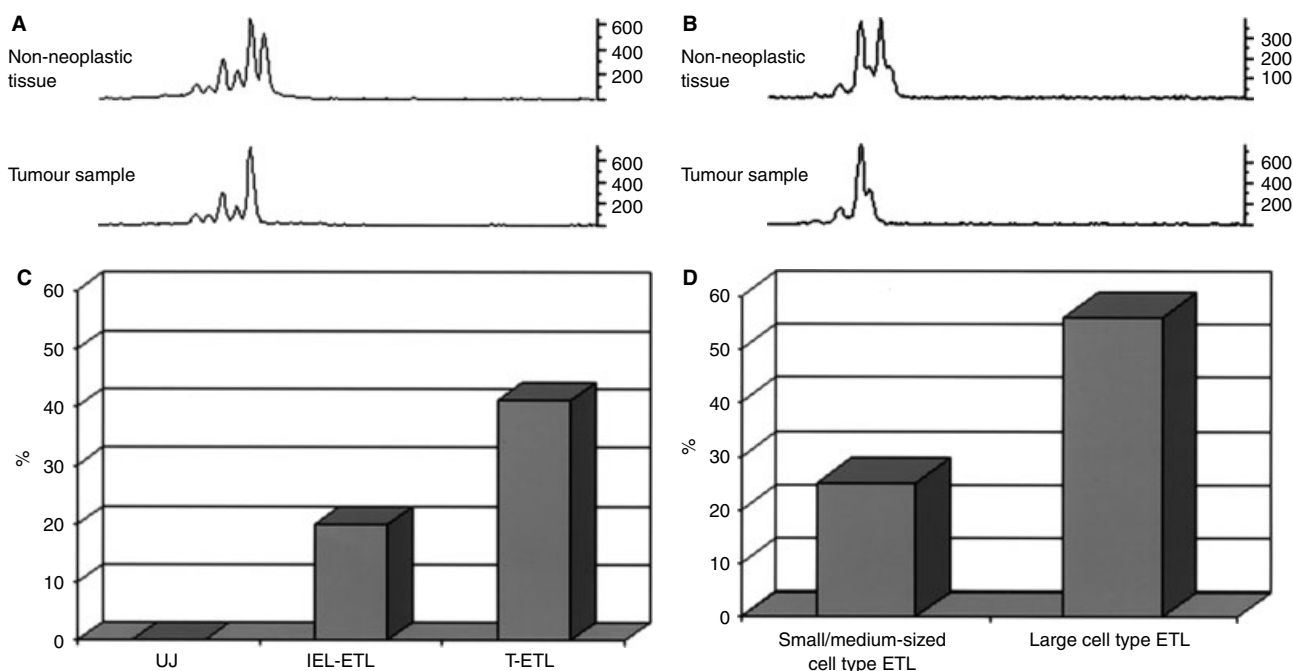


Figure 2. LOH at chromosome 9p21. (A, B) LOH at chromosome 9p21. Two alleles are present in non-neoplastic tissue, while only one allele can be seen in the corresponding tumour sample. (A) IEL-ETL, microsatellite marker p15/p16; the calculated allele ratio is 0.02 (case 10). (B) T-ETL with small-sized cell morphology, microsatellite marker D9S1604; the calculated allele ratio is 0.13 (case 13; see Figure 1D for corresponding loss of p16 expression). (C, D) Percentage of LOH at chromosome 9p21 in different categories. (C) Ulcerative jejunitis, IEL-ETL, and T-ETL. (D) Small- and medium-sized cell type ETL versus large cell type ETL

In this first study to utilize LOH analysis for the investigation of tumour suppressor genes in ETL and UJ, we encountered LOH at 9p21 in 36% of cases. As deletions in this region often include the entire interferon gene cluster, the p15 and p16 gene locus, and the methylthioadenosine phosphorylase gene [31], we chose a broad set of 12 markers extensively covering this region. A similar set of markers spanning the region between D9S161 and D9S144 (located telomeric from IFNa) has been used to investigate p15/INK4b and p16/INK4a in B-NHLs [22].

The core region most intimately linked to the p14/p15/p16 gene loci (from D9S1604 to D9S1747) [28,32,33] was targeted by LOH in five patients with ETL. In all of these cases, loss of nuclear p16 protein expression was observed in more than 90% of neoplastic cells. This finding suggests that LOH in this region is functionally significant. A similar good correlation between genetic changes at 9p21 and lack of p16 protein expression has been observed previously in lymphomas of B-cell origin [22]. Immunohistochemistry could be used to assess the inactivation status of p16 and may serve as a practical substitute for the genetic analysis. The fact that the two cases with LOH further centromeric of the core region had retained p16 expression might suggest that alterations at these loci do not influence p16 expression. Other authors have suggested the presence of a different tumour suppressor gene in this region [33]. Alternatively, as LOH only affects one allele, the remaining allele might be sufficient to maintain p16 protein expression if it is not inactivated by different mechanisms. However, even if no other alterations of the remaining allele occur, a gene dosage effect might have a significant functional influence [34].

LOH at 9p21 was almost exclusively found in overt tumours of ETL. Only in one case (case 29) was LOH found in the main tumour and the accompanying ulceration. Furthermore, only one of five IEL-ETLs and none of the examined cases of UJ showed LOH. There are two possible explanations for this finding. LOH at 9p21 may be a late event in the pathogenesis of ETL, being present mainly in advanced stages with an overt tumour. Alternatively, LOH might occur in IEL-ETL and UJ as demonstrated in case 10, but could be under-detected in other cases due to contamination with normal cells, since the crude microdissection method used in this study could not eliminate these intermingling cells within the neoplastic cell population. The observed loss of nuclear p16 protein expression in the IEL of two UJ cases without demonstrable LOH at 9p21 supports the second hypothesis.

LOH at 9p21 was most frequently encountered in tumours of ETL with large cell morphology; 56% of these cases, as opposed to 25% of cases composed of small- or medium-sized cells, showed LOH. Tumours composed of anaplastic cells particularly displayed LOH at 9p21. One case with anaplastic cells (case 26) did not show LOH: here, the intraepithelial/ulcerated component had been evaluated due to the lack of

material from the main tumour. The contaminating non-neoplastic cells might have obscured the detection of LOH in this case.

Our findings of LOH at 9p21 in ETL is consistent with the study of Zettl *et al* [15], who encountered a loss of genetic material at this region by CGH. The discrepancy in the frequency (36% in LOH analysis versus 18% in CGH analysis) can be explained by the higher sensitivity of the LOH methodology in detecting smaller deletions.

LOH at 9p21 was found in 19% of the other lymphoma entities investigated in our study, as opposed to 36% of ETLs. Although alterations of p15 and p16 are thought to play a role in the pathogenesis of T-cell lymphoma [35,36], data on LOH analysis of 9p21 are rare. So far, cutaneous lymphomas have been investigated for LOH at 9p21; LOH at this locus was found in 25% of mycosis fungoides, 37% of Sezary syndrome [32], and 64% of cutaneous large cell lymphomas [37]. It remains to be investigated whether deletions at 9p21 have prognostic value in UJ and ETL.

Apart from deletions of chromosome 9p21, there are other mechanisms that can inactivate the tumour suppressor genes at this locus. Promotor methylation can lead to transcriptional repression and has been frequently detected for p14, p15, and p16 in both B- and T-cell lymphomas [38]. Somatic mutations of these genes could also silence the transcriptional activity, but are rarely found in lymphomas (eg refs 32, 39, and 40). Homozygous deletions are important for complete inactivation of tumour suppressor genes [17]. It is possible that in some cases in our study the failure of PCR amplification at some microsatellite loci might be due to a homozygous deletion. Quantitative PCR using an internal control gene could address this problem [41]. Alternatively, the amplification of DNA from non-neoplastic bystander cells might obscure both LOH and a homozygous deletion, which is especially likely in UJ, where a high number of inflammatory cells are always part of the lesion. Therefore, both LOH and other inactivation mechanisms of the p16 gene might have led to the loss of p16 protein expression in two cases of UJ. However, as none of the cases of ETL in which we did not detect LOH showed loss of p16 protein expression, we assume that in these cases the region of the p16 gene was not targeted by LOH or other alterations that could impair its function.

In line with the previous report by Murray *et al* [14], we found p53 protein overexpression in the vast majority of cases of UJ and ETL. However, neither LOH nor somatic mutations were demonstrated for the p53 gene. Our molecular data are supported by the study of Zettl *et al* [15], who did not find loss of genetic material at chromosome 17p by CGH. A lack of correlation between p53 gene mutation and p53 protein expression has frequently been reported (eg refs 37, 42, and 43), suggesting additional mechanisms influencing p53 expression. Wild-type p53 may be stabilized by other proteins such as MDM2 [44] and by viral proteins such as SV40 large T cell antigen or HPV type 16 E6

protein [45]. The possibility of p53 stabilization due to alterations in the regulatory p14/ARF–MDM2 loop is intriguing, but p53 stabilization has been observed in the absence of genetic mutations and alterations of p14/ARF [46]. The underlying cause of p53 protein accumulation in ETL and whether the expressed protein is functionally active remain to be investigated.

In summary, we found that LOH on chromosome 9p21 is a frequent finding in ETL, especially in cases with large cell morphology. LOH at the core region of the p16 gene spanned by the microsatellite markers D9S1604 to D9S1747 coincides with the lack of nuclear expression of the p16 protein. Despite frequent overexpression of the p53 protein, alterations of the p53 gene were not detected in UJ or ETL.

Acknowledgements

This work was supported by a Stipendium of the Deutsche Krebshilfe/Dr Mildred Scheel Stiftung für Krebsforschung, Germany and by the Leukaemia Research Fund, UK.

References

- Isaacson P, Wright D. Intestinal lymphoma associated with malabsorption. *Lancet* 1978; **1**: 76–70.
- Isaacson PG, O'Conner NTG, Spencer J, *et al.* Malignant histiocytosis of the intestine: a T-cell lymphoma. *Lancet* 1985; **2**: 688–691.
- Ashton-Key M, Diss TC, Pan L, Du MQ, Isaacson PG. Molecular analysis of T-cell clonality in ulcerative jejunitis and enteropathy-associated T-cell lymphoma. *Am J Pathol* 1997; **151**: 493–498.
- Jewell DP. Ulcerative enteritis. *Br Med J* 1983; **287**: 1740–1741.
- Bagdi E, Diss TC, Munson P, Isaacson PG. Mucosal intraepithelial lymphocytes in enteropathy-associated T-cell lymphoma, ulcerative jejunitis, and refractory celiac disease constitute a neoplastic population. *Blood* 1999; **94**: 260–264.
- Chott A, Vesely M, Simonitsch I, Mosberger I, Hanak H. Classification of intestinal T-cell neoplasms and their differential diagnosis. *Am J Clin Pathol* 1999; **111**: 68–74.
- Wright DH, Jones DB, Clark H, Mead GM, Hodges E, Howell WM. Is adult-onset coeliac disease due to a low-grade lymphoma of intraepithelial T lymphocytes? *Lancet* 1991; **337**: 1373–1374.
- Cellier C, Delabesse E, Helmer C, *et al.* Refractory sprue, celiac disease and enteropathy-associated T-cell lymphoma. *Lancet* 2000; **356**: 203–208.
- Farstad IN, Johansen FE, Vlatkovic L, *et al.* Heterogeneity of intraepithelial lymphocytes in refractory sprue: potential implications of CD30 expression. *Gut* 2002; **51**: 372–378.
- Isaacson PG. Relation between cryptic intestinal lymphoma and refractory sprue. *Lancet* 2000; **356**: 178–179.
- De Bruin PC, Connolly CE, Oudejans JJ, *et al.* Enteropathy-associated T-cell lymphomas have a cytotoxic T-cell phenotype. *Histopathology* 1997; **31**: 313.
- Pan LX, Diss TC, Peng HZ, *et al.* Epstein Barr virus (EBV) in enteropathy associated T-cell lymphoma (EATL). *J Pathol* 1993; **170**: 137–143.
- Quintanella-Martinez L, Lome-Maldonado C, Ott G, *et al.* Primary non-Hodgkin's lymphoma of the intestine: high prevalence of Epstein–Barr virus in Mexican lymphomas as compared with European cases. *Blood* 1997; **89**: 644–651.
- Murray A, Cuevas EC, Jones DB, Wright DH. Study of the immunohistochemistry and T cell clonality of enteropathy-associated T cell lymphoma. *Am J Pathol* 1995; **146**: 509–519.
- Zettl A, Ott G, Makulik A, *et al.* Chromosomal gains at 9q characterize enteropathy-type T-cell lymphoma. *Am J Pathol* 2002; **161**: 1635–1645.
- Sherr CJ. The Pezcoller lecture: cancer cell cycles revisited. *Cancer Res* 2000; **60**: 3689–3695.
- Cairns P, Polaszik TJ, Eby Y, *et al.* Frequency of homozygous deletion at p16/CDKN2 in primary human tumors. *Nature Genet* 1995; **11**: 210.
- Quelle DE, Zindy F, Ashmun RA, Sherr CJ. Alternative reading frames of the INK4a tumor suppressor gene encode two unrelated proteins capable of inducing cell cycle arrest. *Cell* 1995; **83**: 993–1000.
- Pomerantz J, Schreiber-Argus N, Liegeois NJ, *et al.* The Ink4a tumor suppressor gene product, p19ARF, interacts with MDM2 and neutralizes MDM2's inhibition of p53. *Cell* 1998; **92**: 713–723.
- Stott FJ, Bates S, James MC, *et al.* The alternative product from the human CDKN2A locus, p14ARF, participates in a regulatory feed-back loop with p53 and MDM2. *EMBO J* 1998; **17**: 5001–5014.
- Navas IC, Ortiz-Romero PL, Villuendas R, *et al.* p16(INK4a) gene alterations are frequent in lesions of mycosis fungoides. *Am J Pathol* 2000; **156**: 1565–1572.
- Elenitoba-Johnson KSJ, Gascoyne RD, Lim MS, Chhanabai M, Jaffe ES, Raffeld M. Homozygous deletions at chromosome 9p21 involving p16 and p15 are associated with histological progression in follicle center lymphoma. *Blood* 1998; **91**: 4667–4685.
- Jaffe ES, Harris NL, Stein H, Vardiman JE (eds). *World Health Organization Classification of Tumours. Pathology and Genetics of Tumours of Haematopoietic and Lymphoid Tissues*. IARC Press: Lyon, 2001.
- Du MQ, Peng H, Liu H, *et al.* Bcl10 gene mutation in lymphoma. *Blood* 2000; **95**: 3885–3890.
- McCarthy KP, Sloane JP, Kabarowski JHS, Matutes E, Wiedemann LM. A simplified method of detection of clonal rearrangements of the T-cell receptor- γ chain gene. *Diagn Mol Pathol* 1992; **1**: 173–179.
- Goudi RB, Karim SN, Mills K, Alcorn M, Lee FD. A sensitive method of screening for dominant T cell clones by amplification of T cell gamma gene rearrangements with the polymerase chain reaction. *J Pathol* 1990; **162**: 191–196.
- Du M, Peng H, Singh N, Isaacson PG, Pan L. The accumulation of p53 abnormalities is associated with progression of mucosa-associated lymphoid tissue lymphoma. *Blood* 1995; **86**: 4587–4593.
- Heyman M, Rasool O, Borgonov-Brandter L, *et al.* Prognostic importance of p15/INK4b and p16/INK4 gene inactivation in childhood acute lymphocytic leukemia. *J Clin Oncol* 1996; **14**: 2289–2294.
- Gyapay G, Morissette J, Vignal A, *et al.* The 1993–1994 Genethon human genetic linkage map. *Nature Genet* 1994; **7**: 246–339.
- Lakhani SR, Slack DN, Hamoudi RA, Collins N, Stratton MR, Sloane JP. Detection of allelic imbalance indicates that a proportion of mammary hyperplasia of usual type are clonal, neoplastic proliferations. *Lab Invest* 1996; **74**: 129–135.
- Olopade OI, Pomykala HM, Hagos F, *et al.* Construction of a 2,3-megabase yeast artificial chromosome contig and cloning of the human methylthioadenosine phosphorylase gene from the tumor suppressor region on 9p21. *Proc Natl Acad Sci U S A* 1995; **92**: 6489–6493.
- Scarlsbrick JJ, Woolford AJ, Calonje E, *et al.* Frequent abnormalities of the p15 and p16 genes in mycosis fungoides and Sezary syndrome. *J Invest Dermatol* 2002; **118**: 493–499.
- Pollock PM, Welch J, Hayward NK. Evidence for three tumor suppressor loci on chromosome 9p involved in melanoma development. *Cancer Res* 2001; **61**: 1154–1161.
- Venkatachalan S, Shi YP, Jones SN, *et al.* Retention of wild-type p53 in tumors from p53 heterozygous mice: reduction of p53 dosage can promote cancer formation. *EMBO J* 1998; **17**: 4657–4667.

35. Whittaker S. Molecular genetics of cutaneous lymphomas. *Ann N Y Acad Sci* 1993; **941**: 39–45.
36. Liggett WH, Sidransky D. Role of the p16 tumor suppressor gene in cancer. *J Clin Oncol* 1998; **16**: 1197–1206.
37. Boni R, Xin H, Kamarashev J, et al. Allelic deletion at 9p21–22 in primary cutaneous CD30+ large cell lymphoma. *J Invest Dermatol* 2000; **115**: 1104–1107.
38. Baur AS, Shaw P, Burri N, Delacretaz F, Bosman FT, Chaubert T. Frequent methylation silencing of p15INK4b(MTS2) and p16INK4a(MZS1) in B-cell and T-cell lymphomas. *Blood* 1999; **94**: 1773–1781.
39. Pinyol M, Hernandez L, Martinez A, et al. INK4/ARF locus alterations in human non-Hodgkin's lymphomas mainly occur in wild-type p53 gene. *Am J Pathol* 2000; **156**: 1987–1996.
40. Sanchez-Beato M, Saez AI, Navas IC, et al. Overall survival in aggressive B-cell lymphomas is dependent on the accumulation of alterations in p53, p16, and p27. *Am J Pathol* 2001; **159**: 205–213.
41. Berggren P, Kumar R, Sakano S, et al. Detecting homozygous deletions in the CDKN2A(p16(INK4a))/ARF(p14(ARF)) gene in urinary bladder cancer using real time quantitative PCR. *Clin Cancer Res* 2003; **9**: 235–242.
42. Sanchez-Aguilera A, Sanchez-Beato M, Garcia JF, Prieto I, Polan M, Piris MA. P14ARF nuclear overexpression in aggressive B-cell lymphomas is a sensor of malfunction of the common tumor suppressor pathways. *Blood* 2002; **99**: 1411–1418.
43. Oka T, Sarker AB, Teramoto N, Yoshino T, Akagi T. p53 protein expression in non-Hodgkin's lymphomas is infrequently related to p53 gene mutation. *Pathol Int* 1998; **48**: 15–21.
44. Keleti J, Quezado MM, Abaza MM, Raffeld M, Tsokos M. The mdm2 oncoprotein is overexpressed in rhabdomyosarcoma cell lines and stabilizes wild-type p53 protein. *Am J Pathol* 1996; **149**: 143–150.
45. Taylor D, Koch W, Zahurak M, Shah K, Sidransky D, Westra W. Immunohistochemical detection of p53 protein accumulation in head and neck cancer: correlation with p53 gene alterations. *Hum Pathol* 1999; **30**: 1221–1225.
46. Takemoto S, Trovato R, Cereseto A, et al. p53 stabilization and functional impairment in the absence of genetic mutation or the alteration of the p14ARF–MDM2 loop in *ex vivo* and cultured adult T-cell leukaemia/lymphoma cells. *Blood* 2000; **95**: 3939–3944.